OPEN ACCESS Freely available online

AFM Applied Functional Materials

ISSN 2737-5323
Volume 1, Issue 1
https://www.iikii.com.sg/journal/AFM
Applied Functional Materials

Article

Using Different Methods to Measure the Optical Energy Bandgap of Un-annealed and Annealed Ga_2O_3 Films

Ting-Yu Lin [1], Sang-Yuan Han [1], Cheng-Yi Huang [2], Cheng-Fu Yang [1,3]* and Sufen Wei [4,*]

[1] Department of Chemical and Material Engineering, National University of Kaohsiung, Kaohsiung 811, Taiwan; tom110113119@gmail.com (T. U. Lin); qwer1234tyui@gmail.com (S.Y. Han); cfyang@nuk.edu.tw (C. F. Yang)
[2] Department of Electrical Engineering, National Cheng Kung University, Tainan 701, Taiwan; 0309352@gmail.com
[3] Department of Aeronautical Engineering, Chaoyang University of Technology, Taichung 413, Taiwan
* Correspondence: cfyang@nuk.edu.tw, 200961000013@jmu.edu.cn

Received: May 21, 2021; **Accepted:** Jul 2, 2021; **Published:** Aug 30, 2021

Abstract: In this study, electron beam (E-beam) was used to deposit Ga_2O_3 films on the sapphire (Al_2O_3) substratest, then Ga_2O_3 films were divided three groups, unannealed, annealed at 850 ºC, and annealed at 950 ºC, respectively. After that, three different methods were investigated to find the optical energy bandgap of un-annealed and annealed Ga_2O_3 films. First was used n&k analyzer to measure all the optical energy bandgaps of un-annealed and annealed Ga_2O_3 films directly; Second, all the measured transmittance spectra of un-annealed and annealed Ga_2O_3 films, then the cut wavelength at the zero transmittance ratio of the extrapolated straight line according the slope of the absorption edge was used to measure optical energy bandgap using the equation of Eg= 12400/cut wavelength. Third, the curve of $(\alpha h\nu)^2$ against the energy ($h\nu$) value was plotted according to Eqs. $\alpha h\nu = C (h\nu - Eg)^{1/2}$ and $T = (1 - R)^2 \exp(-\alpha d)$, and the extrapolated straight line was used to measure the optical energy bandgap of un-annealed or annealed Ga_2O_3 films. Finally, the measured results were well compared.

Keywords: Different methods; Optical energy bandgap; Un-annealed and annealed; Ga_2O_3 films

1. Introduction

Semiconductive power switching devices with high power and high efficiency are strongly required by today s[oc]iety, because these devices contribute to worldwide energy reduction and conservation. SiC and GaN are representatives of wide-bandgap semiconductors and they have attractive material properties for the applications in power device, for example, their breakdown electric fields and energy bandgaps are larger than those of Si-based devices, therefore, they are expected to overcome the limitation of Si-based devices [1]. Recently, Ga_2O_3-based semiconductors have attracted many researches and become a new competitor to GaN- and SiC-based devices, because Ga_2O_3 films are another wide-bandgap material, and they recognized as another important next generation materials to fabricate power devices. Ga_2O_3-based films also have some significant characteristics, for example, their energy bandgaps are larger than those of GaN- and SiC-based devices [2, 3]. Ga_2O_3-based materials have five different crystal types, which are denoted by α, β, γ, δ, and ∈ [4], and the β-Ga2O3 is the most stable phase, the other four phases are recognized as the intermediate phases and they are unstable as the temperature raises.

Many different methods and substrates are used to deposit β-Ga_2O_3 films. For example, the plasma-assisted molecular beam epitaxy method to the β-Ga_2O_3 films on single crystals of β-Ga_2O_3,GaN, and sapphire under different parameters to epitax the pure-phase β-Ga_2O_3 films [5]. Winkler et al. used a water-based chemistry solution as precursor and the spraying process as a method to deposit the homogeneous nanocrystalline Ga_2O_3 films on commercial fluorine-doped tin oxide (FTO), tin-doped indium oxide (ITO), and spray pyrolysis deposited Indium zinc oxide (IZO) substrates [6]. Wheeler et al. used a plasma-enhanced atomic layer deposition (PEALD) method to grow the Ga2O3 film on sapphire substrates. They found that PEALD is an energy-enhanced and conformal synthesis method, and this method has many advantages, including improved crystallinity, access to metastable phases, and reduced growth temperatures [7]. The β-type crystal has the monoclinic β-gallia structure. Because it is the most stable Ga_2O_3 phase and the other phases are metastable phase during the heating process of Ga_2O_3, therefore, it is the only crystal structure available for the growth of Ga_2O_3-based single crystal.

Mnay methods were investigated the Ga_2O_3 films and used the deposited Ga_2O_3 films to fabricate a metal-insulator-semiconductor (MIS) diode or a thin-film transistor (TFT). For example, Hao et al. used $Ga(OH)_3$ solution as precursor used the liquid-phase deposition (LPD) method to the α-GaOOH crystal film. After the α-GaOOH crystal was obtained by the decomposition

of the $Ga(OH)_3$ solution, the post annealing process was used to transform the α-GaOOH into the α-Ga_2O_3 crystal. Then, Hsieh et al. used the deposition α-Ga_2O_3 film to fabricate a MIS diode [8]. Thomas et al.used an ultrasonic spray pyrolysis method to grown the Ga_2O_3 film at 400–450 ºC in ambient atmosphere, then they annealed the deposition Ga_2O_3 film at different temperatures to find their optimum properties. Then, they used the annealed Ga_2O_3 film and using heavily doped Si^{++} wafer as the common gate electrode to fabricate a bottom-gate, top-contact TFT [9].

The reported energy bandgaps of β-Ga_2O_3 are widely distributed in the range of 4.4–4.9 eV [1-3, 10], which is caused by the complexity of optical processes in Ga_2O_3-based materials. Thus, the really energy bandgaps of β-Ga_2O_3 are difficult to confirm, and in this study, we had investigated three different methods to measure the energy bandgaps of β-Ga_2O_3 films. Because Ga_2O_3 films were deposited using E-beam method and deposition Ga_2O_3 films presented amosphorous, therefore, we needed to anneal deposited Ga_2O_3 films at the high temperatures of 850 and 950 ºC to transform amosphorous Ga_2O_3 films into the β-Ga_2O_3 films. As we know, n&k analyzer is a multi-functional equipment because it can measure refractive index, the extinction coefficient, the optical energy bandgap, the reflectance spectrum, the transmittance spectrum, and thickness of a deposition film at the same time. Therefore. the first method is that n&k analyzer was used to measure all the optical energy bandgaps of un-annealed and annealed Ga_2O_3 films directly. Second, after all the transmittance spectra of un-annealed and annealed Ga_2O_3 films were measured, then, we uesd the cut wavelength at the zero transmittance ratio of the extrapolated straight line according the slope of the absorption edge to measure optical energy bandgap using the equation of Eg= 12400/(cut wavelength). Third, we would plot the curve of $(\alpha h\nu)^2$ against the energy (hν) value according to Eqs. $\alpha h\nu = C\ (h\nu - Eg)^{1/2}$ and $T = (1 - R)^2 \exp(-\alpha d)$, and the extrapolated straight line was used to measure the optical energy bandgap of un-annealed or annealed Ga_2O_3 films. Then, the average optical energy bandgaps of five samples measured using three different methods were compared in this study.

2. Materials and Methods

At first, the pure Ga_2O_3 (99.99%) was sintered at 1200 °C to fabricate Ga_2O_3 target. After the sapphire (Al_2O_3) substrates were cleaned, electron-beam (E-beam) evaporation method was used to deposit Ga_2O_3 film. The deposition parameters of Ga_2O_3 film were that the working pressure in the vacuum chamber was set at 3 x 10^{-3} Torr, the distance between substrate and target was about 60 cm, room temperature (RT) was used as the deposition temperature, respectively, and no gas was introduced into the chamber during the deposition process. Because we wanted transform the amorphous Ga_2O_3 films intoβ-Ga_2O_3 films, therefore we needed to anneal deposited Ga_2O_3 films at the high temperatures of 850 and 950ºC, the sapphire (Al_2O_3) substrates were used to dposit the Ga_2O_3 films [11]. Next, n&k analyzer was used to measure the optical energy bandgaps and the transmittance spectra of un-annealed and annealed Ga_2O_3 films, the transmission spectra of un-annealed and annealed Ga_2O_3 films were measured in the wavelength 2range of 300–800 nm. The thickness of deposited Ga_2O_3 films was controlled at approximately 150 nm by controlling the deposition time. The XRD pattern was used to analyze the crystalline phase of un-annealed and annealed Ga_2O_3 films. A field emission scanning electron microscope (FESEM) was used to observe the surface morphology and to confirm the thickness of deposited Ga_2O_3 film.

3. Results

There are six differently crystalline phases existing in the Ga_2O_3, including α, β, γ, δ, ε, and κ phases [12]. Playford et al. used a low-cost liquid-phase deposition (LPD) method to prepare the Ga_2O_3 precursor and they found that all the γ-Ga_2O_3, δ-Ga_2O_3, ε-Ga_2O_3, and κ-Ga_2O_3 were intermediate phases and they were unstable as the temperature is raised. For example, δ-Ga_2O_3 phase was transformed into ε-Ga_2O_3 phase at temperature higher than 400 ºC; γ-Ga_2O_3, ε-Ga_2O_3, κ-Ga_2O_3, and α-Ga_2O_3 phases were transformed into β-Ga_2O_3 phase as the temperatures are higher than 550 ºC, 500 ºC, 500 ºC, and 700 ºC, respectively. Thus, as compared with those results of Playford et al., annealed Ga_2O_3 films had different results. XRD patterns of un-annealed Ga_2O_3 film and 850 ºC- and 950 ºC-annealed Ga_2O_3 films are show in Figure 1 as a function of annealing temperature. As Figure 1 shows, no apparent diffraction peak was observed in un-annealed Ga_2O_3 film, this results suggests that un-annealed Ga_2O_3 film was amorphous phase rather than other crystalline phase. Figure 1 also shows that the different diffraction peaks were presented in 850 ºC- and 950 ºC-annealed Ga_2O_3 films, which suggest that the crystallinity of Ga_2O_3 films is improved as the annealing procees is used to treat on deposition Ga_2O_3 films. When the annealing temperature was 850 ºC, the mainly crystalline phase was the ε-Ga_2O_3 phase, and the β-Ga_2O_3 phase was also observed; when the annealing temperature was raised to 950 ºC, the only crystalline phase was the the β-Ga_2O_3 phase, the ε-Ga_2O_3 phase was not observed. As-deposited Ga_2O_3 films possess mostly amorphous phase and they can be transformed into polycrystalline β-Ga_2O_3 phase after annealing treatment when the temperature was higher than 850 °C. However, the annealing treatment is a more helpful process to improve the crystal qualities of Ga_2O_3 films.

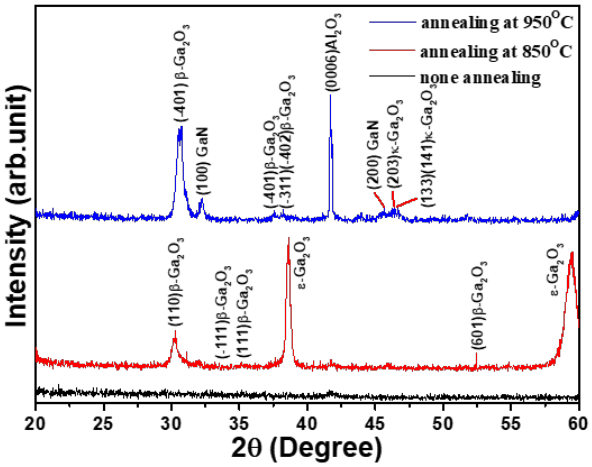

Figure 1. XRD patterns of Ga_2O_3 films as a function of annealing temperature.

Figures 2(a)-(c) show the surface observations of Ga_2O_3 films as a function of annealing temperature, all the surfaces of un-annealed and annealed Ga_2O_3 films present a nanocrystalline structure and revealled a smooth and densified structure. As the annealing temperatures of Ga_2O_3 films raised from RT to 850 ºC and 950 ºC, as the surface morphologies in Figures 2(a), 2(b), and 2(c) show, the morphologies and grain sizes of Ga_2O_3 films had different results as the annealing temperature was raised. The crystallite sizes of Ga_2O_3 films were not observed in unannealed Ga_2O_3 film and they were really observed in the 850 ºC- and 950 ºC-annealed Ga_2O_3 films. These results in Figure1 and Figsure 2(a)-2(c) have proven that the annealing temperature has large effect on the surface morphologies and crystallization of Ga_2O_3 films and then it has large effect on the optical properties of Ga_2O_3 films. These results presented in Figure 2 suggest that as annealing temperature raised, the Ga_2O_3 film had the better crystallinity, which matched the variation of XRD patterns presented at Figure 1.

Even the crystallite sizes were observed in the 850 ºC- and 950 ºC-annealed Ga_2O_3 films, their sizes were not easily to be measured from the observed SEM micrographs. Therfore, we used the Scherrer formula to calculate the crystallite sizes of 850 ºC- and 950 ºC-annealed Ga_2O_3 films [13], the average particle sizes were 17.8 and 21.4 nm as the annealing temperatures were 850 ºC and 950 ºC, respectively. The results in Figure (1) and Figure (2) prove again that the annealing temperature has large effects on the crystalline phases and the average particle sizes of Ga_2O_3 films. Thus, we prove again that the annealing temperature will have large effect on the opticall properties of Ga_2O_3 films, that is proven in the following paragraphs. The cross-sectional thickness of deposited Ga_2O_3 film was also observed and the result was shown in Figure 2(d), which shows the thickness of deposited Ga_2O_3 film was about 155 nm, and all the thicknesses of un-annealed and annealed Ga_2O_3 films were in the ranges of 148~158 nm.

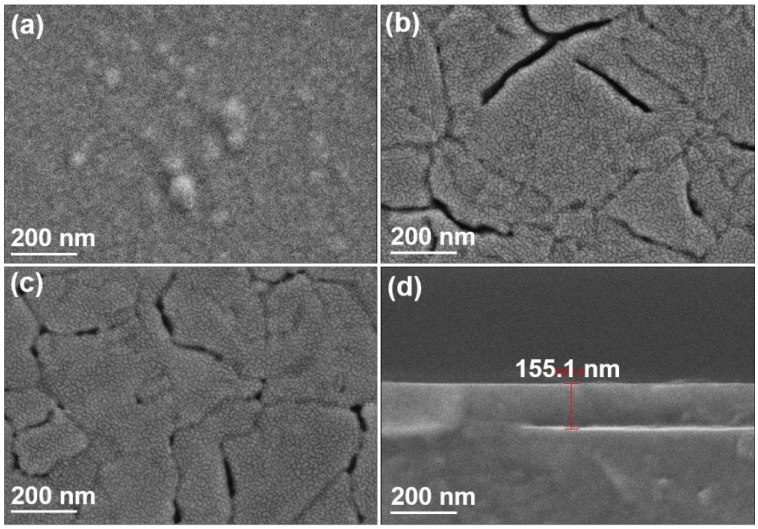

Figure 2. SEM micgrgraphs of Ga_2O_3 films (a) un-annealed, (b) annealed at 850 ºC, (c) annealed at 950 ºC, and (d) cross-sectional observation.

When n&k analyzer was directly used to measure the optical energy bandgaps of un-annealed Ga_2O_3 film and 850ºC- and 950ºC-annealed Ga_2O_3 films, the measured values were 2.99, 4.86, and 5.71 eV, respectively. These results suggest that the optical energy bandgaps of un-annealed and annealed Ga_2O_3 films increased with annealing temperature. These results also suggest that the optical energy bandgap of β-Ga_2O_3 phase is larger than those of amphorous Ga_2O_3 phase and ε-Ga_2O_3 phase. Transmittance spectra of un-annealed, 850 ºC-annealed, and 950 ºC-annealed Ga_2O_3 films are shown in Figure 3(a), Figure 4(a), and Figure 5(a), respectively. All the transmittance ratios of un-annealed and annealed Ga_2O_3 films were very low because the sapphire substrate are one kind of material with low transparency. The saturation transmittance ratios of un-annealed and annealed Ga_2O_3 films were approximately 12%, which suggests the annealing temperature had no apparent effect on the maximum transmittance ratio of un-annealed and annealed Ga_2O_3 films. When the transmission spectra shown in Figure 3(a), Figure 4(a), and Figure 5(a) were compared, we found that for for un-annealed Ga_2O_3 film, the transmittance ratio increased slightly and reached the saturation value at about wavelength of approximately 600 nm.

Thus, for 850 ºC- and 950 ºC-annealed Ga_2O_3 films, the transmittance ratio increased critically in a narrow range of wavelength. These results suggest that un-annealed Ga_2O_3 film has many defects, which will decrease the transmittance ratio at lower wavelengths of 300-500 nm, and crystallized Ga_2O_3 films have less defects and they have apparent absorption edges. We also had found that when the annealing temperature raised from RT to 950ºC, the extrapolated straight lines at transmittance ratios of 0% and the absorption edges and of Ga_2O_3 films had been shifted to the lower wavelengths. The absorption edges and of Ga_2O_3 films shown in Figure 3(a), Figure 4(a), and Figure 5(a) were 248.5, 220.1, and 202.1 nm. When we used 1240 nm to divide by the 248.5, 220.1, and 202.1 nm, the optical energy bandgaps were 4.99 (in the range of 4.92~5.05), 5.63 (5.54~5.74), and 6.14 (6.06~6.19) eV, respectively. These results prove again that the optical energy bandgap of β-Ga_2O_3 phase is larger than those of amphorous Ga_2O_3 phase and ε-Ga_2O_3 phase.

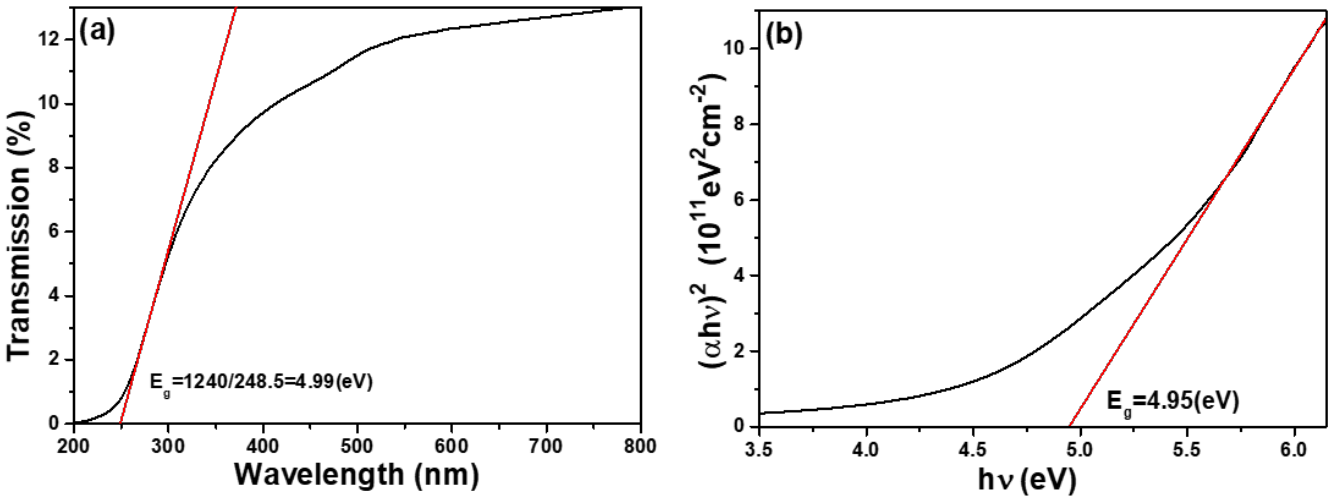

Figure 3. (a) Transmittance spectrum and (b) $(\alpha h\nu)^2$ vs hν (energy) plots of un-annealed Ga_2O_3 film.

The following two equations could be used to calculate the relationship of optical energy bandgap (E_g) and absorption coefficient (α) of un-annealed and annealed Ga_2O_3 films: [14,15]

$$T = (1 - R)^2 \exp(-\alpha d) \qquad \alpha h\nu = C\,(h\nu - E_g)^{1/2} \quad (1)$$

where T, R, C, $h\nu$, and d are transmittance ratio, reflectance ratio, a constant, light energy, and thickness of measured film, respectively. The curves of energy value ($h\nu$) against the $(\alpha h\nu)^2$ values are calculated and plotted according to Eq. (1), and the extrapolated straight lines were used to measure the optical energy bandgap of un-annealed and annealed Ga_2O_3 films. The results of un-annealed, 850 ºC-annealed, and 950 ºC-annealed Ga_2O_3 films are shown in Figure 3(b), Figure 4(b), and Figure 5(b), respectively. When the annealing temperatures were RT, 850 ºC, and 950 ºC, the optical energy bandgaps of un-annealed, 850 ºC- annealed, and 950 ºC-annealed Ga_2O_3 films were 4.95 (in the range of 4.88~5.02), 5.27 (5.21~5.33), and 5.52 (5.45~5.58) eV, respectively. However, we found that no matter which method is used, the optical energy bandgaps of Ga_2O_3 films increased with annealing temperatures. These results prove again that the optical energy bandgap of β-Ga_2O_3 phase is larger than those of amphorous Ga_2O_3 phase and ε-Ga_2O_3 phase, even the the optical energy bandgaps of Ga_2O_3 films measured in this study are larger than the measured results in other researches. These results in this study also show an important conclusion that the

optical energy bandgaps of β-Ga_2O_3 films using the extrapolated straight lines of the plotted curves of energy value ($h\nu$) against the $(\alpha h\nu)^2$ values are more close to other researches.

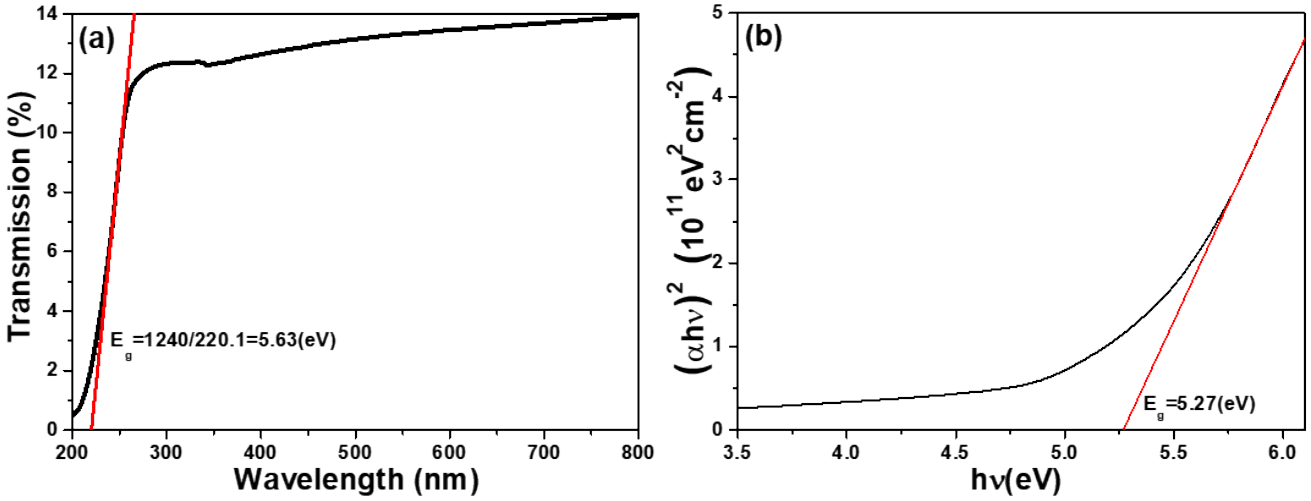

Figure 4. (a) Transmittance spectrum and (b) $(\alpha h\nu)^2$ vs hν (energy) plots of 850 ºC-annealed Ga_2O_3 film.

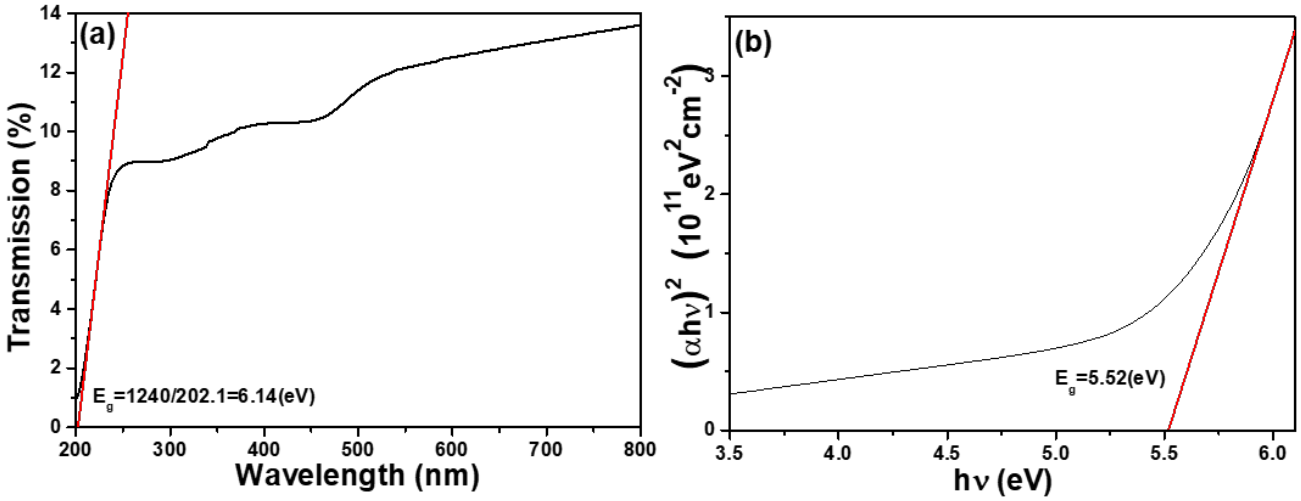

Figure 5. (a) Transmittance spectrum and (b) $(\alpha h\nu)^2$ vs hν (energy) plots of 950 ºC-annealed Ga_2O_3 film.

5. Conclusions

In this study, three methods were successfully investigated to find the optical energy bandgaps of un-annealed Ga_2O_3 film and 850 ºC- and 950 ºC-annealed Ga_2O_3 films. When n&k analyzer was directly used to measure the optical energy bandgaps of un-annealed Ga_2O_3 film and 850 ºC- and 950 ºC-annealed Ga_2O_3 films, the measured values were 2.99, 4.86, and 5.71 eV; When the cut wavelength at the zero transmittance ratio of the extrapolated straight line according the slope of the absorption edge was used, the optical energy bandgaps of un-annealed Ga_2O_3 film and 850 ºC- and 950 ºC-annealed Ga_2O_3 films were 4.99 (in the range of 4.92~5.05), 5.63 (5.54~5.74), and 6.14 (6.06~6.19) eV; When the extrapolated straight lines of the plotted curves of energy value (hν) against the $(\alpha h\nu)^2$ values were used to measure the optical energy bandgaps of un-annealed Ga_2O_3 film and 850 ºC- and 950 ºC- annealed Ga_2O_3 films, the results were 4.95 (in the range of 4.88~5.02), 5.27 (5.21~5.33), and 5.52 (5.45~5.58) eV, respectively.

Author Contributions: For research articles with several authors, a short paragraph specifying their individual contributions must be provided. Conceptualization, T.Y. Lin, C.F. Yang, and S. Wei; methodology, T.Y. Lin, S.Y. Han, C.Y. Huang, C.F. Yang, and S. Wei; formal analysis, T.Y. Lin, S.Y. Han, and C.F. Yang; investigation, T.Y. Lin, C.F. Yang, and S. Wei; resources, C.F. Yang and S. Wei.; data curation, T.Y. Lin, S.Y. Han, and C.F. Yang; writing—original draft preparation, T.Y. Lin, C.Y. Huang, C.F. Yang, and S. Wei; writing—review and editing, C.F. Yang and S. Wei; visualization, T.Y. Lin, S.Y. Han, and C.F. Yang; supervision, T.Y. Lin, S.Y. Han, C.F. Yang, and S. Wei". Authorship must be limited to those who have contributed substantially to the work reported.

Acknowledgments: In this section, you can acknowledge any support given which is not covered by the author's contribution or funding sections. This may include administrative and technical support, or donations in kind (e.g., materials used for experiments).

Conflicts of Interest: The authors declare no conflict of interest.

References

1. Higashiwaki, M.; Murakami, H.; Kumagai, Y.; Kuramata, A. Current status of Ga_2O_3 power devices. *Jpn. J. Appl. Phys* **2019**, *55*, 1202A1.
2. He, H.; Orlando, R.; Blanco, M.A.; Pandey, R.; Amzallag, E.; Baraille, I.; Rérat, M. First-principles study of the structural, electronic, and optical properties of Ga_2O_3 in its monoclinic and hexagonal phases. *Phys. Rev. B* **2006**, *74*, 195123.
3. Onuma, T.; Saito, S.; Sasaki, K.; Masui, T.; Yamaguchi, T.; Honda, T.; Higashiwaki, M. Valence band ordering in β-Ga_2O_3 studied by polarized transmittance and reflectance spectroscopy. *Jpn. J. Appl. Phys* **2015**, *54*, 112601.
4. R. Roy, V. G. Hill, and E. F. Osborn. Polymorphism of Ga_2O_3 and the System Ga_2O_3—H_2O. *J. Am. Chem. Soc* **1952**, *74*, pp. 719-722.
5. Hao, S.J.; Hetzl, M.; Schuster, F.; Danielewicz, K.; Bergmaier, A.; Dollinger, G.; Sai, Q. L.; Xia, C. T.; Hoffmann, T.; Wiesinger, M.; Matich, S.; Aigner, W.; Stutzmann, M. Growth and characterization of β-Ga_2O_3 thin films on different substrates. *J. Appl. Phys* **2019**, *125*, 105701.
6. Winkler, N.; Wibowo, R. A.; Kautek, W.; Ligorio, G.; List-Kratochvil, E. J. W.; Dimopoulos, T. Nanocrystalline Ga_2O_3 films deposited by spray pyrolysis from water-based solutions on glass and TCO substrates. *J. Mater. Chem. C* **2019**, *7*, pp. 69-77.
7. Wheeler, V.D; Nepal, N.; Boris, D.R.; Qadri, S. B.; Nyakiti, L. O.; Lang, A.; Koehler, A.; Foster, G.; Walton, S.G.; Eddy, C. R. Jr.; Meyer. D.J. Phase Control of Crystalline Ga_2O_3 Films by Plasma-Enhanced Atomic Layer Deposition. *Chem. Mater* **2020**, *32*, pp. 1140−1152
8. Hsieh, Y.S.; Li, C.Y.; Lin, C.M.; Wang, N.F.; Li, J.V.; M.P. Houng, M.P. Investigation of metal-insulator-semiconductor diode with alpha-Ga_2O_3 insulating layer by liquid phase deposition. *Thin Solid Films* **2019**, *685*, pp. 414–419.
9. Thomas, S.R.; Adamopoulos, F.; Lin, Y.H.; Faber, H.; Sygellou, L.; Stratakis, E.; Pliatsikas, N.; Patsalas, P.A.; Anthopoulos, T.D. High electron mobility thin-film transistors based on Ga_2O_3 grown by atmospheric ultrasonic spray pyrolysis at low temperatures. *Appl. Phys. Lett*. **2014**, *105*, 092105.
10. Mohamed, M.; Unger, I.; Janowitz, C.; Manzke, R.; Galazka, Z.; Uecker, R.; Fornari, R. The surface band structure of β-Ga_2O_3. *Journal of Physics: Conference Series* **2011**, *286*, 012027.
11. Rafique, S.; Han, L.; Neal, A.T.; Mou, S.; Tadjer, M.J.; French, R.H.; Zhao, H.P. "Heteroepitaxy of N-type β-Ga_2O_3 thin films on sapphire substrate by low pressure chemical vapor deposition". *Appl. Phys. Lett*. **2016**, *109*, 132103.
12. Playford, H.Y.; Hannon, A.C.; Barney, E.R.; Walton, R.I. Structures of uncharacterised polymorphs of gallium oxide from total neutron diffraction. *Chem. Eur. J*., **2013**, *19*, pp. 2803-2813.
13. Chen, C.C.; Wang, F.H.; Chang, S.C.; Yang, C.F. Using Oxygen Plasma Pretreatment to Enhance the Properties of F-Doped ZnO Films Prepared on Polyimide Substrates. *Materials* **2018**, *11*, p. 1501
14. Youn Du, Chih-Cheng Chen, Fang-Hsing Wang, Chun-Chi Lin, Yang, C.F. Effect of deposition temperature and F_2 flow rate on the characteristics of F-doped ZnO films. *Modern Phys. Lett. B* **2019**, *33*, 1940040
15. Lin, Z.J.; Shih, M.C.; Wang, F.H.; Yang, C.F. Study on the properties of zinc oxide films with different CF4 flow rates. *Modern Phys. Lett. B* **2021**, *35*, 2150204.

Publisher's Note: IIKII stays neutral with regard to jurisdictional claims in published maps and institutional affiliations.